Chromatographic Separation of Rare Earth Elements as MGDA Complexes on Anion Exchange Resins

Kurkinen Santeri, Virolainen Sami, Sainio Tuomo

DOI: 10.3390/met13030600

metals

MDPI

Article

Chromatographic Separation of Rare Earth Elements as MGDA Complexes on Anion Exchange Resins

Santeri Kurkinen [1], Sami Virolainen [1,*] and Tuomo Sainio [2]

[1] School of Engineering Science, LUT University, Yliopistonkatu 34, 53850 Lappeenranta, Finland; santeri.kurkinen@lut.fi
[2] School of Engineering Science, LUT University, Mukkulankatu 19, 15210 Lahti, Finland
* Correspondence: sami.virolainen@lut.fi; Tel.: +358-50-431-6756

Abstract: Chromatographic separation of rare earth elements (REE) as anionic complexes with chelating aminopolycarboxylate ligand methylglycine *N*,*N*-diacetate (MGDA) was studied experimentally. A synthetic mixture of La, Nd, and Eu were used to model a REE mixture obtained from processed secondary sources such as phosphogypsum (PG). In the REE extraction from PG, the REEs can be recovered with MGDA to obtain the REE–MGDA mixture. Three strong base anion exchange resins (Dowex 1X8, IRA-402, and IRA-410) were used as the separation materials. Successful separation of the REEs by elution with dilute HNO_3 and HCl was attributed to differences in the stabilities of the REE–MGDA complexes. The pKa values of the complexes were determined by titration to be 3.81, 3.25, and 2.96 for La, Nd, and Eu, respectively. Fractionation of the ternary La-Nd-Eu mixture (with a 1:1:1 mole ratio) were studied. La was recovered at approximately 80% purity and 80% yield, but strong trade-offs between the yield and the purity of Nd and Eu must be made. Chromatographic separation was found to be an efficient process option, considering its simplicity and the recovery of several product fractions. The initial process design offers a promising starting point for investigating more advanced process configurations for the efficient recovery of pure REE from phosphogypsum.

Keywords: rare earth element; chromatography (preparative); anion resin; MGDA; HCl; separation techniques; ion exchange

Citation: Kurkinen, S.; Virolainen, S.; Sainio, T. Chromatographic Separation of Rare Earth Elements as MGDA Complexes on Anion Exchange Resins. *Metals* **2023**, *13*, 600. https://doi.org/10.3390/met13030600

Academic Editor: Guihong Han

Received: 8 February 2023
Revised: 8 March 2023
Accepted: 14 March 2023
Published: 16 March 2023

1. Introduction

Rare earth elements (REEs), especially when considering lanthanides, are known for their similar chemical properties. They all exist commonly in a REE^{3+}-oxidation state, but few of them can also have oxidation states of either REE^{2+} or REE^{4+} [1]. All REEs have partially filled 4f-orbitals, giving them their unique properties due to the phenomenon known as lanthanide contraction. This unique property of the electron shell configuration affects their chemical bonding, further intensifying their chemical similarities [2]. These minor differences between individual lanthanides, scandium, and yttrium result in significant difficulty in the complete separation of these elements. Thus, either highly advanced chemical processes and/or many process cycles are needed to achieve high purities.

Different methods can be used to fractionate lanthanide mixtures to pure single metal fractions or smaller sets of REE (e.g., adjacent REE pairs such as La/Ce, Sm/Eu, and Ce/Pr). These methods include precipitation [3], solvent extraction (SX) [4], ion exchange (IX), and ion chromatography (IC) [5,6]. All these methods have their advantages and disadvantages. Precipitation of REEs is usually performed with a ligand that produces poorly soluble solids, such as oxalate [7]. These precipitation methods usually require precise control of the pH due to small differences in the formation energies of individual REE complexes [8]. The greatest advantage of direct precipitation is an instant solid product, which can easily be turned into oxides. For solvent extraction, the overall separation is not technically difficult, but its downside is its many consecutive steps [9]. In addition, solvent extraction operations

require large-scale use of chemicals (acids, organic solvents, and other chemicals) even though they are usually recyclable [10]. In addition to conventional organophosphorus extractants, new α-aminophosphorous extractants have been developed for REE separation by solvent extraction [11]. The development of solvent extraction separation of REEs in academic literature also deals with ionic liquids [12]. A new kind of separation material has been developed to achieve highly selective REE sorption and separation [13–16]

In the Manhattan project, the IX methods, for example with cation or anion ion exchange, were developed to remove REEs and other valuable elements from the radioactive material [17]. Before IX-based methods, separation was based on the crystallization of pure REE components, which is very time consuming. The IX methods significantly reduced the required time and work [18]. Chromatographic separation has become one of the viable methods for REE separation in addition to solvent extraction. Now, with modern HPLC (High Performance Liquid Chromatography) equipment and materials, the complete separation of REEs from their mixture can be achieved in a single column step [19]. However, the scalability of these kinds of separation systems is limited; the superior separation efficiency of the HPLC in pilot scale or larger is cost intensive. Conventional preparative columns that operate with completely different parameters (pressure, column dimensions, and particle and/or pore size of separation material) are unable to reach a similar level of separation efficiency.

The large variety of chromatographic methods are based on the affinities and interactions between the species to be separated, the stationary phase, and the eluent medium [20]. One of the chromatographic methods is high-speed counter-current chromatography (HSCCC) [21]. Chromatographic separation of REEs can be based on the separation of complexed REEs [22]. One type of complex chromatography is ligand assisted chromatography [23]. Complexation of REEs enhances minor differences in the chemistry of the elements. The complexing agent may or may not be chelating if they result in a complex with a charge. The largest difference is that chelating agents tend to form more stable complexes than non-chelating ones. These kinds of complexing compounds include amino(poly)carboxylic acids (EDTA (ethylenediaminetetraacetic acid), IDA (iminodiacetic acid, NTA (nitrilotriacetic acid), MGDA) and (poly)carboxylic acids (citric acid, acetic acid). Separation can be achieved with both cation and anion resins, depending on the charge of the complex formed. A suitable eluent combined with the right resin enables selective separation of REEs with a known order relative to their complex stabilities and properties [24,25]. REE mixtures can be introduced to the chromatographic system either as free ions or complexes. Cation exchange resins can be used when the feed contains REE as free cations or positively charged complexes. Free cations are sorbed to the resin, then released from the resin with suitable eluent (complexing agent, acid, etc.). Anion resins can be used in the opposite situation, where the REE feed or the separation material has been pre-treated with a complexing agent. Preferably these negatively charged species are usually pushed through the chromatographic system using a complexing agent as the mobile phase [26,27]. This kind of separation usually requires large quantities of the mobile phase relative to the amount of complex present in the system [28]. Table 1 reviews several methods from the literature that achieved partial or complete REE separation. In most of the previous methods, separation was achieved using HPLC equipment and/or eluents that are expensive or highly concentrated.

Table 1. Examples of REE separations using chromatographic methods.

Resin Material, Particle Size	Resin Bed Dimensions	Mobile Phase and Concentration	Fed REE vs. Column Size [g/L]	HPLC/ Preparative	Ref.
Dowex 2X8 (200–400 mesh)	d = 1.2 cm h = 36 cm	Sodium trimetaphosphate [≤10 mM]	0.12	Preparative	[29]
AS9-HC	d = 0.4 cm h = 25 cm	EDTA [5 mM]	0.0032	HPLC	[26]
C18 coated silica [1] d = 16 µm	d = 0.46 cm h = 15 cm	Nitric acid [7 M]	1.96	HPLC	[30]
Eternity XT5–C18	d = 0.46 cm h = 25 cm	TBAOH [8.6 mM]/ODA [5 mM]	0.00012–0.00036	HPLC	[31]

[1] The C18 column was further functionalized with HDEHP before use.

In this work, the separation of REEs in the form of the MGDA complex is studied. The study proposes a novel process to separate anionic MGDA-REE complexes with dilute acid as mobile phase. MGDA-REE complexes originated from resin-in-leach recovery of REE from phosphogypsum [32]. In addition to the complexation of REE with MGDA, the combination of anion IX resin as a sorbent and the dilute acid as the mobile phase make the studied unit process novel for the separation of pure REEs from their mixture. Due to the anionic nature of MGDA-REE complexes, the cation IX resins were not considered as a separation material. Dilute acid as the mobile phase in this separation can reduce the chemical load compared to systems with alkaline complexing agents (e.g., EDTA). The effect of feed composition, resin type, acid type, and temperature are explored with a synthetic MGDA-REE solution. The purpose of synthetic feed is to determine the factors that are affecting the separation of the MGDA-REE complex without the presence of impurities. The effect of impurities for separation efficiency is not discussed, although in realistic case minor levels of impurities would exist in the feed. The separation of MGDA-REE complexes with a conventional packed resin bed without the use of HPLC technology will enable us to proceed towards techno-economically efficient REE recovery from phosphogypsum. The novelty of this work is that the separation of REEs is achieved with dilute HCl while the anion IX resin acts as a separation material and not with the use of a complex forming ligand in the mobile phase. This results in a new method for REE separation, which could be a more economically viable option for separation since it uses dilute HCl as the eluent, which is cheap compared to the ligand-based (for example MGDA) mobile phases.

2. Materials and Methods

2.1. Anion Exchange Resins

The IX resins used were Dowex 1X8, IRA-402 and IRA-410. Dowex 1X8 is a strong base anion (SBA) exchanger with quaternary ammonium as functional groups and 8% DVB (divinylbenzene) content. IRA-402 is similar; it consists of SBA resin with quaternary ammonium groups and a 6% DVB content. Dowex 1X8 and IRA-402 are both type I resins. Additionally, IRA-410 is a type II resin with dimethylethanolamine functional groups. The structures of the functional groups for both type I and type II resins are shown in Figure 1. In addition, the structure of MGDA (the complexing ligand used in this study) is shown on the same figure. The physical and chemical properties of the selected resins are shown in Table 2.

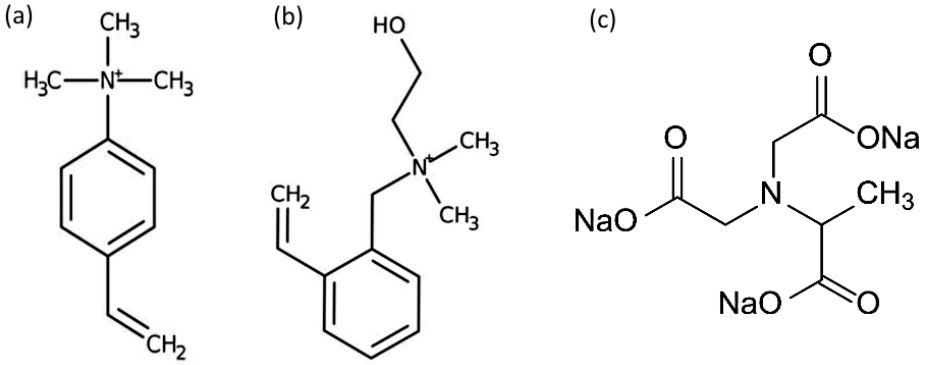

Figure 1. Functional groups of (**a**) Dowex 1X8 and IRA-402; (**b**) IRA-410; (**c**) MGDA-Na_3.

Table 2. Physical and chemical properties of the resins used in this study.

Resin	Dowex 1X8	IRA-402	IRA-410
Functional group	$N^+(CH_3)_3$	$N^+(CH_3)_3$	$N^+(CH_3)_2C_2H_4OH$
Matrix	PS-DVB	PS-DVB	PS-DVB
Structure	gel	gel	gel
DVB Content, wt-%	8	6	8
Particle size, mm	0.6–0.75	0.6–0.75	0.6–0.75

2.2. Synthetic Feed Solutions

The chemicals used in this study were HCl (CAS: 7647-01-0) (VWR Chemicals, Briare, France, 36%, GPR Rectapur), HNO_3 (CAS: 7697-37-2) (Merck, Darmstadt, Germany, 65%, Analysis purity), H_2SO_4 (CAS: 7664-93-9) (VWR Chemicals, Briare, France, 96%, GPR Rectapur), MGDA (CAS: 164462-16-2), (Honeywell Fluka, Seelze, Germany, ≥90%), $LaCl_3 \cdot 7\ H_2O$ (CAS: 10025-84-0) (Fluka Chemika, Seelze, Germany, Puriss. p.a.), Nd_2O_3 (CAS: 1313-97-9) (Sigma-Aldrich, Taufkirchen, Germany, 99.9%), and Eu_2O_3 (CAS: 1308-96-9) (Sigma-Aldrich, Taufkirchen, Germany, 99.9%)

The feed simulates the real MGDA-REE product that was previously obtained from authentic industrial phosphogypsum waste by eluting REE-loaded resin with the alkaline MGDA solution [32]. REEs in the loaded resin originated from an authentic industrial phosphogypsum waste that was treated with a cross-current ion exchange resin-in-leach process. The feed solutions were prepared by dissolving solid rare earth chemicals. Solids were dissolved by concentrated HCl, then diluted with water. Although selected REE solids are also soluble in other minerals acids (HNO_3 and H_2SO_4), HCl was selected because it has the fewest unfavorable interactions with REEs and SBA, (i.e., a low affinity towards the resin and REE in a complex formation) [33,34]. The main negative effect of HCl is its corrosive effect on the used equipment. HNO_3 affects the resin matrix (nitration) and chelating MGDA ligand negatively (oxidizing) and H_2SO_4 was rejected due to its double anion formation (HSO_4^- and SO_4^{2-}) and strong affinity towards both type I and type II SBA resins.

The total REE concentration of the prepared stock solution was 0.3 M, and it was used for preparing all the feed solutions. The pH adjustments were done either with HCl or NaOH, if needed. The ratio of individual REEs in stock solution was 1:1:1 (±5%), as it allows to detect selectivity and affinity differences more easily. The composition and properties of the feed solutions are shown in Table 3. Solutions were prepared by mixing REE stock solution (0.3 M) with solid MGDA–Na3 salt. For most samples, the REE:MGDA stoichiometric ratio was 1:1 since their dominant complex structure is 1:1 [32], and complexation is estimated to be very strong at this ratio (i.e., the majority of the REE and MGDA are in complexes). In addition, the 1:1 ratio of REE:MGDA does not allow resin to transform to the MGDA-form since nearly all of it is in REE–MGDA complexes. To study the effect of excess MGDA in the sample, a feed with a 1:4 REE–MGDA stoichiometric ratio was also prepared. The pH of the samples was adjusted to be slightly alkaline to

ensure the complex formation between the ligand and REE since the MGDA is an acid with pKa values pKa_1 = 9.9; pKa_2 = 2.6, and pKa_3 = 1.5 [35]. Regardless of the high pH of feed solutions, the REEs are not in the form of hydroxide precipitate in the solution. Chelation with MGDA alters the solution chemistry of REE cations and they exist as water soluble MGDA-REE complexes within the pH range of 9 to 12.50. Deviations in feed concentrations between each other are due to the pH adjustments of the feed. NaOH or HCl addition to the feed caused an increase in volume of the feed and thus resulted in lower concentration of REE (g/L). The starting point for pH adjustments was on the alkaline level (pH = 12.5), so therefore the lower pH values ended up having lower concentrations of REE due to added HCl.

Table 3. Compositions of the feed solutions used in the experiments.

Feed Number	∑(REE) [g/L]	pH	[REE]:[MGDA]
1	28.4	12.20	1:1
2	29.6	12.45	1:1
3	21.6	9.08	1:1
4	19.5	9.81	1:4

2.3. Chromatographic System

The anion exchange resins were pretreated with multiple consecutive HCl and NaOH cycles to remove any traces of impurities before use. Twenty grams of wet resin was slurry-packed into a glass column (Kronlab ECO101382, ID = 15 mm). The bed height varied between 20.0 and 21.5 cm, depending on the resin. The bed was supported from above and below using variable-length adaptors. The temperature of the packed bed was controlled, if needed, with a water jacket connected to the thermostat. Experiments that were done in ambient temperature (298 ± 2 K) did not have additional temperature control. No significant shrinking or swelling of the particles were observed during the process with any of the eluents.

The resins were used in the same ion form as the major anion in the mobile phase in each experiment (Cl^-, SO_4^{2-} or NO_3^-). Before each experiment, the column was regenerated with a concentrated acid solution (HCl, H_2SO_4, or HNO_3) and equilibrated with the mobile phase (0.01–0.15 mol/L of HCl, H_2SO_4, or HNO_3). The two-step loading-elution experiments were an exception; the column was initially equilibrated with purified water and the eluent was a 0.01–0.05 mol/L HCl solution. The feed was introduced to the column by using injection loops of fixed sizes (0.2–2 mL = 1–10% of BV). Any exceptions to these default initial conditions and procedures are mentioned later in the text.

Samples with a fixed volume (time-based) were collected by fraction collector (Foxy R1) to the plastic tubes. Tubes were closed with caps prior to the analysis. The metal content from the collected fractions was analyzed using offline methods.

2.4. Analytical Methods

For metal (La, Nd, Eu) analysis in the aqueous phase, the Agilent 7900, Basel, Switzerland, inductively coupled plasma mass spectrometer (ICP-MS) was used. The relative standard deviation (RSD) in ICP-MS measurements was ±2%. Measurement of pH was done with Consort multi-parameter analyzer C3010, Turnhout, Belgium, and WTW SenTix Mic pH electrode, Weilheim, Germany. The error estimate for the pH measurements was ±0.1%, one digit, according to the specifications of the manufacturer. MGDA as a free, undissociated acid or its corresponding sodium salt form, was analyzed with Agilent 6560 Ion Mobility LC/Q-TOF. The reverse phase column (Waters Acquity Premier HSS T3, Milford, MA, USA) was selected as the solid phase. The chosen column minimally interacts with metal cations, making it easier to detect free aminopolycarboxylic acids (MGDA).

3. Results and Discussion

3.1. Selection of the Resin and the Mobile Phase

3.1.1. Resin

Figure 2 displays profiles obtained with the Dowex 1X8, IRA-410, and IRA-402 when the REE–MGDA mixture "Feed #2" (Table 3) was eluted through the packed bed with 10 mM HNO_3. In all cases, the elution profile (total REE concentration) consists of two partially separated peaks. Their origin and composition are discussed later in the paper, but the Dowex 1X8 yields inferior separation of the REEs compared to the IRA resins. With the Dowex 1X8, the majority of the REEs are eluted within a large peak at the void volume of the column. The IRA-402 resin, in contrast, exhibits a broader elution profile in which the REEs are mostly retained by the resin. These two resins have the same functional group but differ in cross-linking density (8 wt-% for Dowex 1X8 vs. 6 wt-% for IRA-402). This suggests that 8 wt-% DVB content results in a polymer matrix too dense for the REE–MGDA complexes to penetrate the gel area and reach the functional groups. This is congruent with the findings in previous publications, which studied the separation of EDTA–Ln (Ln = Lanthanide) complexes with, for example, Dowex 1X2 and 1X4 resins [36,37]. In addition, IMDA–Ln complexes were investigated with different Dowex 1X and 2X resins; Dowex 2X8 has been shown to be a suitable resin for REE separation. Sodium trimetaphosphate gradient eluent was used to separate adjacent REEs [29]. In this study the IRA-410 was found to have similar properties to the Dowex 2X8.

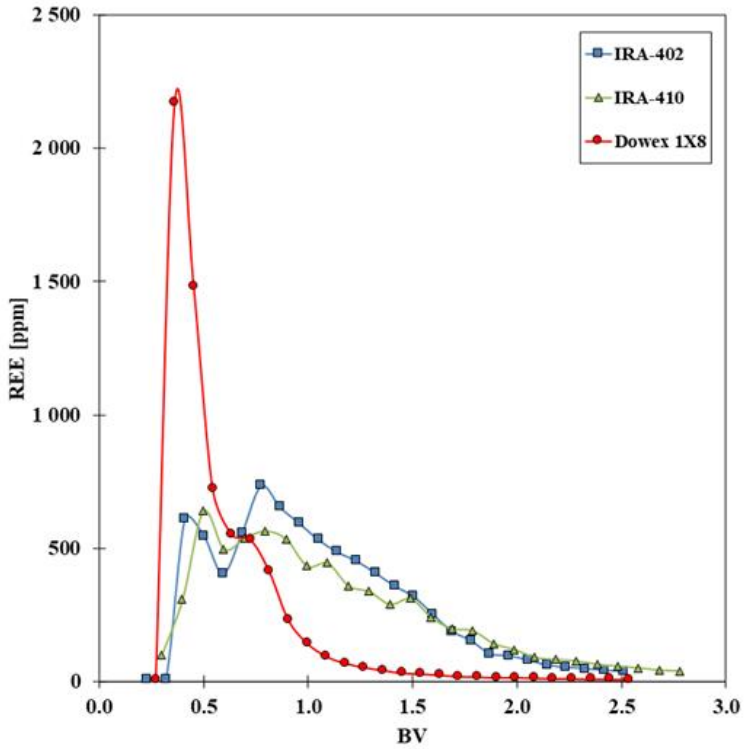

Figure 2. Chromatograms for REE elution with Dowex 1X8, IRA-410 and IRA-402 (T = 298 ± 2 K; flowrate = 2.98 BV/h; feed pulse = 0.025 BV, Eluent = 10 mM HNO_3; Feed solution = #2).

The elution behaviour of REEs was similar for the type I and type II resins (i.e., IRA-402 and IRA-410) even though their cross-link densities are different (8 wt-% with IRA-410). This is readily seen in Figure 3, where the elution profiles of La, Nd, and Eu are shown. Chromatograms were obtained from two separate experiments. The feed contains all three shown REEs mixed, but for comparison purposes they are shown as divided elements (La, Nd, Eu). The Type II resin (IRA-410) shows a stronger retention of Eu (last eluted REE) than the Type I resin, despite its higher DVB content. Therefore, it can be concluded that the Type II functionality in the strong base anion exchanger increases the retention.

Moreover, the retention of La (first eluted REE) on IRA-410 is weaker and the retention of Nd (middle) is like that of IRA-402. Based on these results, IRA-410 yields the best separation of the REEs under these conditions and, therefore, was chosen for most of the subsequent experiments. The selection of the resin is done completely on the empirical basis based on the results of this study.

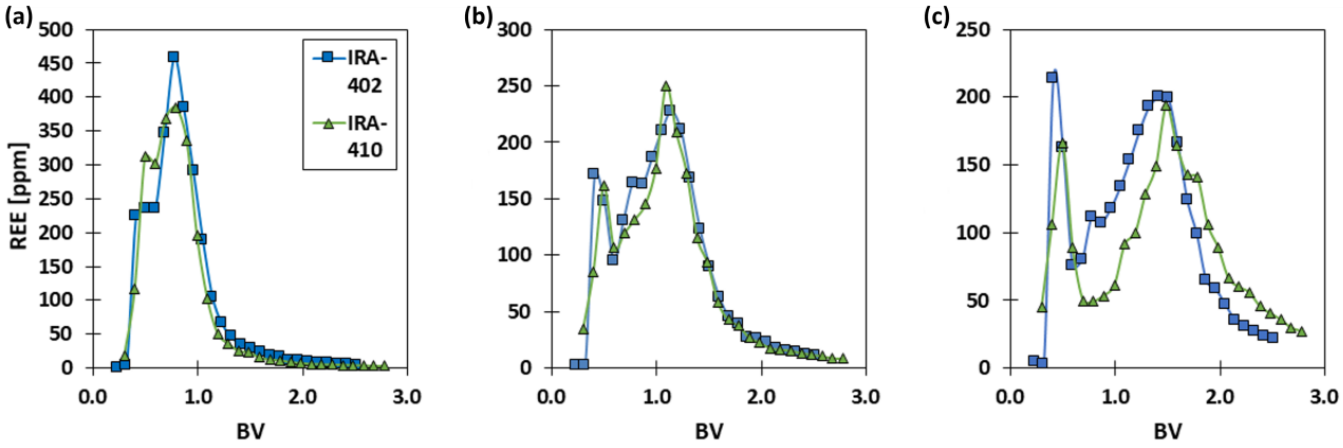

Figure 3. Elution profiles of (**a**) La; (**b**) Nd; and (**c**) Eu on IRA-402 and IRA-410. (T = 298 ± 2 K; flowrate = 2.98 BV/h; feed pulse = 0.025 BV, Eluent = 10 mM HNO_3; Feed solution = #2).

3.1.2. Mobile Phase

Dilute solutions of strong mineral acids were used as the mobile phase in the elution of MGDA–REE complexes for two reasons. Firstly, the acidic eluent weakens the stability and changes the total net charge of the MGDA–REE complexes by protonating at least one of the carboxylic acid groups of the chelating ligand (MGDA). The protonation of functional groups in the resin is not considered. The stability of, for example, the IRA-410 resin, is good for the whole pH range from 0 to 14. Therefore, operating the separation dilute acids does not result in protonation of the functional groups. Secondly, the different anions from the acid compete with the MGDA–REE complex for the functional group of the resin. In this way, the pH and choice of acid could be used to enhance the separation of the REEs with a simple mobile phase.

Common mineral acids used in this type of separation are H_2SO_4, HNO_3, and HCl. Preliminary tests revealed that no separation of REEs is achieved when sulfuric acid is used as the mobile phase, even in small concentrations (10 mM). This stems from the extreme affinity of sulfate and bisulfate towards both type I and type II SBA resins in acidic pH. The use of sulfuric acid results in a persistent sulfate form in the resin, requiring large volumes of suitable salts to convert the resin back to either their Cl^- or NO_3^- form [38]. Therefore, sulfuric acid is an unsuitable mobile phase due to its strong interaction with all types of the resin phase.

The general trend of affinity towards SBA resins is $SO_4^{2-} > NO_3^- > Cl^-$. There is a notable difference in the affinities of NO_3^- and Cl^- to Type I and Type II resins when OH^- is used as the reference. For Type I resins, the selectivity coefficients are in the following order: $K_{OH^-}^{Cl^-}$ = 22 and $K_{OH^-}^{NO_3^-}$ = 65 for Type I resins, and $K_{OH^-}^{Cl^-}$ = 2.2 and $K_{OH^-}^{NO_3^-}$ = 8 for Type II resins [34]. The Type I resin is less selective to NO3- than the Type II resin ($K_{Cl^-}^{NO_3^-}$ = 2.95 vs. $K_{Cl^-}^{NO_3^-}$ = 3.49). It is expected that these affinity differences would cause variations in the elution behavior of different REE–MGDA complexes with different mineral acids.

Disqualification of H_2SO_4 as a mobile phase leaves us with two options: HNO_3 and HCl. Figure 4 shows that HNO_3 results in slightly lower retention, but the separation of peaks is not that great. Respectively, with HCl, the retention of metals increases, and the profiles are broader. Generally, using HNO_3 with an anion exchange resin as the mobile phase is not recommended since it might undergo nitration, oxidizing the resin

matrix. Therefore, HCl is chosen to be the most suitable eluent for REE. This minimizes the interaction between the MGDA–REE complex and anions present in the mobile phase. The formation constant of, for example, an $NdCl_x$ complex in Cl–medium is low compared to the formation constants of the MGDA–REE complex at an alkaline pH. At 25 °C, β_1 and β_2 for $NdCl^{2+}$ and $NdCl_2^+$ are (0.28) and (no value), respectively. Based on the formation constants of REE-Cl_x ($x \geq 1$) complexes, these complexes are not significantly present in dilute chloride solutions [33].

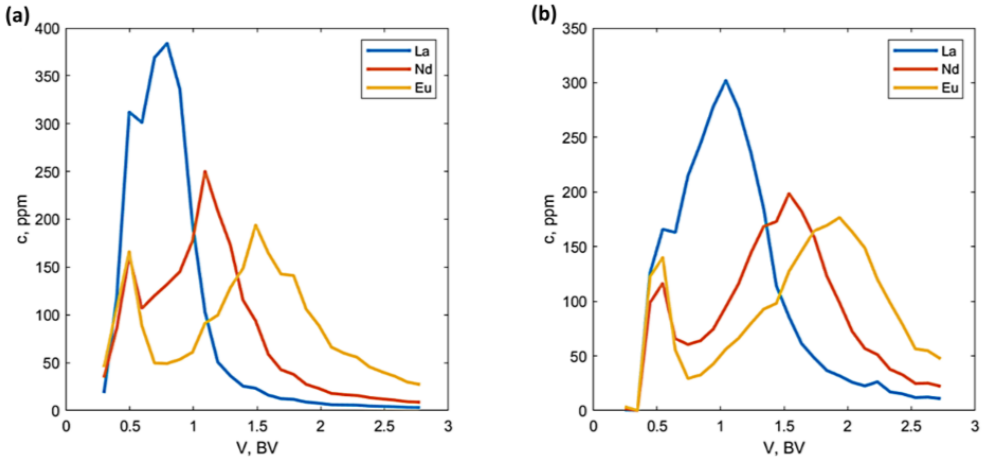

Figure 4. Separation of REEs on IRA-410 using (**a**) HNO_3 and (**b**) HCl as the eluent (T = 298 ± 2K; flowrate = 2.98 BV/h; feed volume = 0.025 BV; acid concentration = 10 mM).

3.2. Sorption Behavior of REE

A 1:1 REE–MGDA complex has a net negative charge in an alkaline solution (pH ≥ 9). Due to its negative charge, the complex is capable of binding to the SBA resin's functional groups. The sorption equilibrium is affected by the solution pH, the REE:MGDA ratio, and the temperature. In almost every chromatogram in this study, a sharp peak of REEs around 0.5 BV can be seen. This will be discussed in more detail later. With the used resins and mobile phases (eluents), the frontal peak cannot be removed. The flow rate and feed volume could affect the extent of separation achieved in the column, but these were not investigated because a more comprehensive process design and the effect of feed volume will be examined in future work.

3.2.1. The Effect of Temperature on REE Separation

The temperature was found to have a small effect on the separation of the REE–MGDA complexes (Figure 5). Increasing the temperature enhanced the sorption of the MGDA–REE complexes. Higher temperatures caused the resin matrix to become more flexible and swollen, allowing for better mass transfer and enhancing the kinetics, which can be seen as a slightly faster process cycle. This caused a decrease in the size of the frontal peak group at the beginning of the chromatogram. The REE mass balance shifted to the right towards the second peak group, where we observe the retention of the MGDA-REE complexes. Temperature did not have noticeable effect on the desorption or retention. Higher temperatures than ambient (22 °C) could be used in the loading step of a two-step process to enhance the sorption of the MGDA–REE complex.

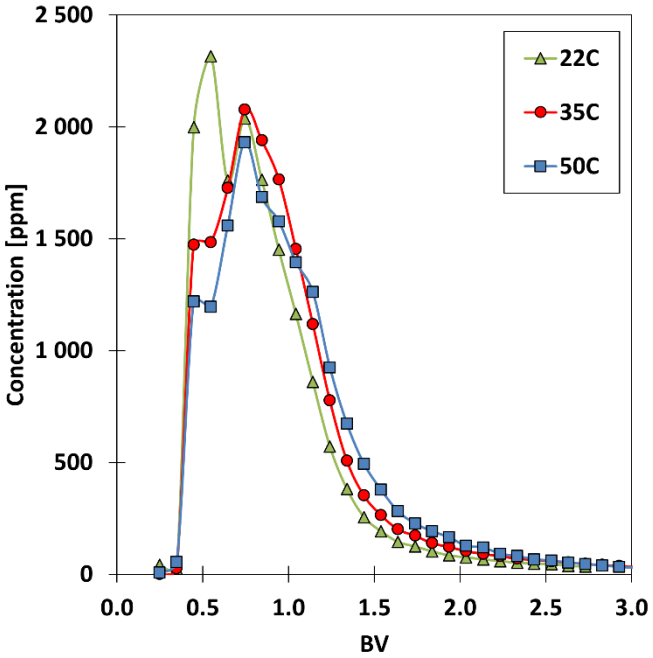

Figure 5. Effect of temperature on the retention of the MGDA–REE complexes shown as Σ[REE] (resin = IRA–410; flowrate = 2.98 BV/h; feed (#2) = 0.05 BV, eluent = 50 mM HCl).

3.2.2. Effect of the Acid Concentration on REE Separation

The effect of HCl concentration on the retention of MGDA–REE complexes is shown in Figure 6. All REEs are eluted faster when the HCl concentration increases from 0.01 M to 0.05 M; additionally, the peaks become sharper. This results in higher peak concentrations for every REE. However, the peaks significantly overlap. Overlapping becomes more severe with the increasing acid concentration. Evidently, 0.05 M HCl is already too acidic to achieve good separation of the REEs. On the other hand, concentrations lower than 0.01 M are not suitable because the MGDA–REE complexes already have a high retention with 0.01 M HCl; it would cause long process cycle times and low productivity. For an isocratic process, the mobile phase of 0.01 M HCl with pH = 1.92 was deemed suitable even though the Eu profile spreads widely. For sharper elution and smaller retention of the MGDA–Eu complex, a pH buffer gradient could be used as the eluent.

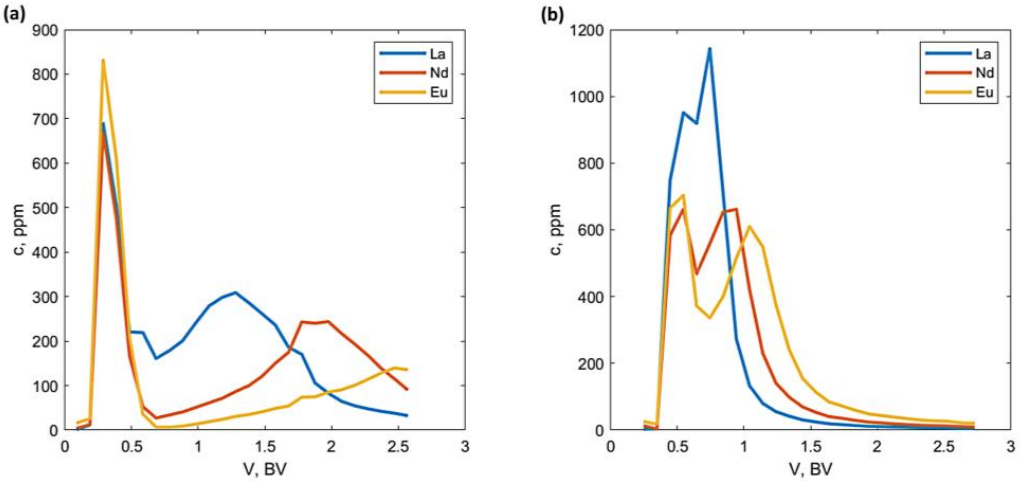

Figure 6. Effect of HCl concentration in the eluent on the retention behavior of REEs on IRA-410: (**a**) 10 mM HCl; (**b**) 50 mM HCl (flowrate = 2.98 BV/h; feed solution = #2; feed volume = 0.05 BV).

3.2.3. Effect of the Feed pH on REE Separation

For a substantial number of the experiments, the initial pH of the feed pulse was greater than 12. Highly alkaline conditions were selected to ensure complexation of REEs with MGDA (pKa_1 = 9.9; pKa_2 = 2.6; pKa_3 = 1.5). A high pH also ensures negative charge of the complex, which is needed for the sorption to an SBA resin. The pH of the feed pulse decreases soon after injecting it into the column because the column was equilibrated with an acidic mobile phase. In the case of a water equilibrated column, the pH of the outcoming feed does not change drastically based on the pH values measured from the effluent fractions (Figure S1). A high feed pH is an important factor to ensure the sorption of the MGDA–REE complexes on the anion exchange resin [39].

The use of feed with a pH between 9 and 10 (Feeds 3 and 4) resulted in different retention behavior for La and Nd complexes than with pH 12 (Figure 7). Due to the lower pH of the feed (pH = 9), the MGDA–La complex is almost immediately affected by the acid content of the column. This neutralized and partly protonated MGDA-La complex does not show any retention. La can be seen as a single sharp peak at the beginning of the chromatogram that does not tail significantly. The retention behavior of Nd has also changed. The position of the peak has shifted to the right in the chromatogram. Overall, the peak shape and its width is similar to feed with a pH of 12.20 (Figure 7). Since the MGDA–La complex does not interact with the resin's functional groups, the MGDA–Nd complex is the first to interact with the mobile phase after the feed has been injected to the column. In addition, the lower initial pH of the feed can contribute to altered retention. Retention of the MGDA-Eu complex did not change with the varied pH of the feed.

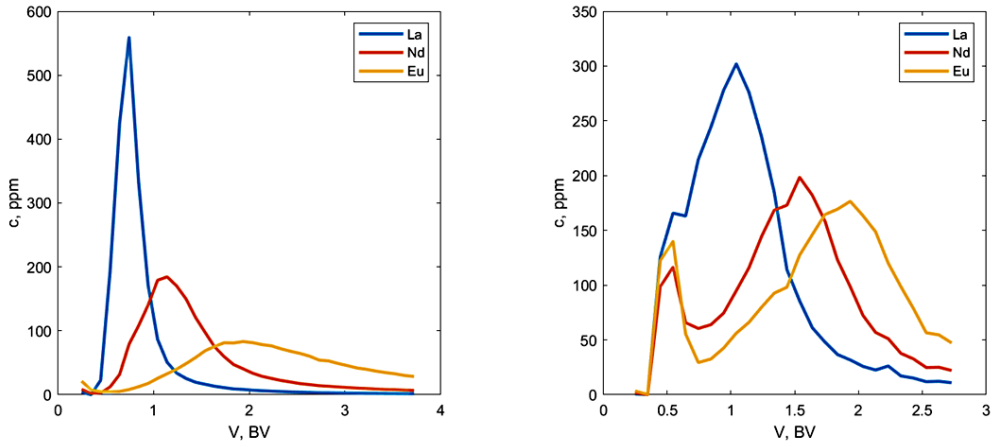

Figure 7. Chromatogram with feed pH = 9.08 (**left**) and feed pH = 12.20 (**right**) (resin = IRA-410; T = 298 ± 2 K; flowrate = 2.98 BV/h; feed pulse = 0.025 BV; acid concentration = 10 mM).

Further acidification of the feed would also change the retentions of the MGDA–Nd and MGDA–Eu complexes. A more acidic feed would render MGDA–REE complexes chargeless, or the complex would at least lose the negative charge that is needed for interaction with the resin phase.

3.2.4. Effect of the MGDA–REE Ratio on REE Separation

MGDA–REE complexes exist mainly with a molar ratio of 1:1. A molar ratio between MGDA and REE larger than 1:1 has an excess of MGDA. Having a large excess of MGDA in the alkaline feed solution transforms the SBA resin partly to its MGDA form because the free MGDA's negatively charged carboxylic acid groups interact with the resin. Having the SBA resin in the same form as the complexing ligand decreases the distribution factors. It was observed that having chloride resin resulted in a better distribution factor compared to the MGDA resin. However, having the resin in the form of a complexing agent can significantly increase the working capacity of the resin. The working capacity is determined from the breakpoint, describing the number of complexes that are capable of sorbing to the

SBA resin in a dynamic process. An increase in the working capacity results in a decrease in the total capacity of the resin [40]. An increase in the working capacity compensates for lower distribution factors by allowing for more complexes into the system during the dynamic process. This results in greater retention of the MGDA–REE complexes.

Figure 8 shows the experiment with a 4:1 MGDA–REE ratio. This excess of the chelating ligand can be observed as a stronger retention of all MGDA–REE complexes than with a 1:1 MGDA–REE ratio (Figure 4). This results in a wide and low peak shape. Increasing the working capacity when using excess ligand in the feed solution creates a small frontal peak. This peak is significantly larger in the case of a 1:1 ratio between MGDA and REE. The general trend does not differ drastically from the experiments with an equivalent amount of MGDA and REE in the feed.

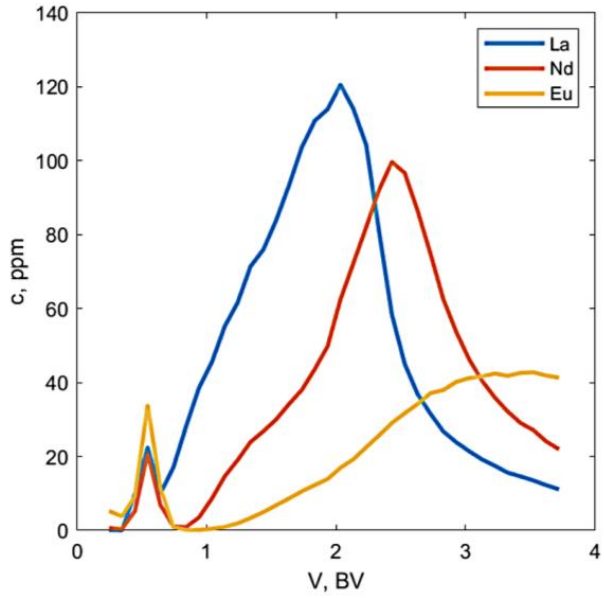

Figure 8. The chromatogram of the experiment with a feed solution having a 4:1 MGDA–REE ratio. (resin = IRA–410; T = 298 ± 2 K; flowrate = 2.98 BV/h; feed (#4) = 0.025 BV; eluent = 10 mM HCl).

3.3. Stability of the MGDA–REE Complexes

MGDA–REE complexes are stable within a large pH range, and they have a negative net charge in alkaline conditions. This negative charge and consequent electrostatic interaction with the functional group of the SBA resin is the main sorption mechanism. As discussed earlier, the separation is based on the differences between the complex stabilities of individual REE–MGDA complexes. Based on the structure of the MGDA molecule, the -COO^- located near the methyl group is the most sensitive to protonation. The methyl group acts as an electron density donor, which destabilizes the -COO^- and results in protonation of the acid group. Alkyl substituents are known to be electron density donors and, thus, induce a higher pKa value in the adjacent -COOH group [41].

3.3.1. Titration of the MGDA–REE Complexes

The differences between the complex stabilities were investigated with a simple titration method. For titration purposes, the REEs (La, Nd, Eu) were complexed with MGDA individually. Initial pHs of the samples were set to 10.5 (>pKa_3 = 9.9) when the MGDA forms stable chelate with REE. These samples were then titrated with 0.1 M HCl. The equilibrium point is observed as a gentle slope in the pH/dV curve (Figure 9). The results verify our assumption of the protonation of at least one of the carboxylic acid groups. Values for the first pKa of the MGDA–REE complex can be determined from the equivalent points of the titration curve. The value for the MGDA–La complex is significantly higher than that of the MGDA–Nd and MGDA–Eu complexes. The complex

strengths have an order of La < Nd < Eu, which is in line with the order of the metals in the periodic table; complex strength is inversely proportional to the size of the ion. A decrease in the ionic radius results in more stable complexes [42]. REEs are known for their lanthanide contraction, which results in an atypical size of the ion when the mass of the ion increases [2]. The differences in pKa values between REE–MGDA complexes result in differences in the free energy of adsorption. The La complex with the largest pKa value determined gives a ΔG° (Gibbs free energy of adsorption) of −21.51 kJ/mol. The values of ΔG° for Nd and Eu are −18.30 kJ/mol and −16.67 kJ/mol, respectively. A larger negative free energy of adsorption indicates stronger interaction with the resin. This can be seen in the ratios between La, Nd, and Eu in the front peak. The Eu, which has the weakest interaction with the resin, has a larger share in the front peak compared to the original feed.

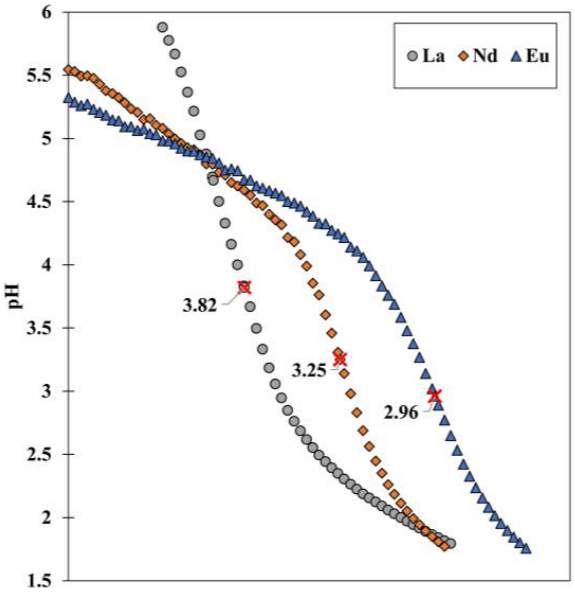

Figure 9. Titration curves of the individual MGDA-REE complexes. The pKa values of the equivalent points are marked on the titration curves. Grey = La (3.82), orange = Nd (3.25), blue = Eu (2.96) (titrant = 10 mM HCl; fixed speed titration; T = 298 ± 2 K).

Interactions between negative MGDA–REE complexes and the positively charged SBA resin further modifies the protonation tendency of MGDA. Electrostatic interactions such as London dispersion forces or ion-induced dipole effects could affect the charge distribution within the MGDA–REE complex [43]. This leads to a higher pKa, where the protonation of the first COO^- occurs. This plausible interaction explains the differences of pH values observed in titration and in the elution process itself.

Differences in complex stabilities can already be seen when the MGDA-REE loaded column is rinsed with water. Deionized water can elute the MGDA–La complex since its pH is 5.8, which is acidic enough to cause partial protonation and neutralization of the MGDA–La complex, thus liberating it from the resin. Since the third pKa values of the MGDA-Nd and MGDA-Eu complexes are significantly lower than that of the MGDA-La complex, those complexes remain sorbed to the resin during the loading and rinsing of the column with water. This small, steady leakage of the MGDA–La complex during water rinsing can be seen in Figure S2.

3.3.2. Presence of Free MGDA in the REE Solution

The majority of the MGDA in the feed was assumed to be in the form of an MGDA–REE complex. This assumption can be justified by the large stability constant of the MGDA–La complex (log K = 11.02; 20 °C) [44]. To prove complex stabilities and their presence in acidic HCl media after chromatographic separation, the amount of the free, non-complexed form of MGDA was determined from the eluent samples. MGDA—either in the form

of undissociated acid (MGDA–H_3) or the corresponding sodium salt (MGDA-Na_3)—are considered to be free ligands. Semi-quantitative LC-MS analysis of effluent samples yielded information regarding the MGDA–REE complex stability. A significant amount of free MGDA compared to the overall concentration of MGDA in the feed would indicate a dissociation of the MGDA–REE complex.

The amount of free MGDA was analyzed with LC-MS analysis. Figure S3 shows the mass spectrum for a pure MGDA–Na_3 feed. One can see both forms of free MGDA (MGDA–H_3 and MGDA–Na_3). In addition, one partly fractionated molecule with m/z = 160 can be seen; this is the result of decarboxylation of the MGDA. Table 4 shows both experimental and theoretical m/z values for the MGDA and its decarboxylated form. Experimental m/z values fit to the theoretical counterparts within an acceptable deviation based on the ΔmDa values.

Table 4. Experimental and theoretical mass-to-charge ratios for measured MGDA forms.

Ion	Formula	*m/z* (Exp.)	*m/z* (Theor.)	ΔmDa
$[MGDA + Na]^+$	$C_7H_{11}NO_6$ + Na	228.0463	228.0479	−1.6
$[MGDA + H]^+$	$C_7H_{11}NO_6$ + H	206.0645	206.0659	−1.4
$[MGDA + H\text{-}COOH]^+$	$C_6H_{10}NO_4$	160.0589	160.0604	−1.5

The actual samples containing complexed MGDA-REE species were analyzed with similar LC-MS analysis for the free MGDA. The amount of free MGDA was assumed to be minimal because the sample's MGDA–REE ratio was 1:1. Higher concentrations are assumed to be seen in samples with a 4:1 MGDA–REE ratio.

Figure 10 displays the ∑REE concentration from one of the experiments combined with the observed relative amounts of free MGDA in a logarithmic scale. The frontal peak group that contains all three REEs in the sample was detected immediately after the injected sample pulse traveled through the void volume of the column (0.4 BV). This narrow part of the chromatogram contains the large majority of the observed free MGDA. The amount of free MGDA is miniscule after the frontal peak group. Both REE and free MGDA concentrations are proportional to each other after the frontal peak group. In fraction #22 (Figure 10), the concentration for MGDA is 10 times smaller than that in fractions #9 and #13 (Figure 10). The concentration of free MGDA based on semi-quantitative analysis shows only µg/L-level concentrations in every sample, while the concentration in the feed was on the mg/L-level.

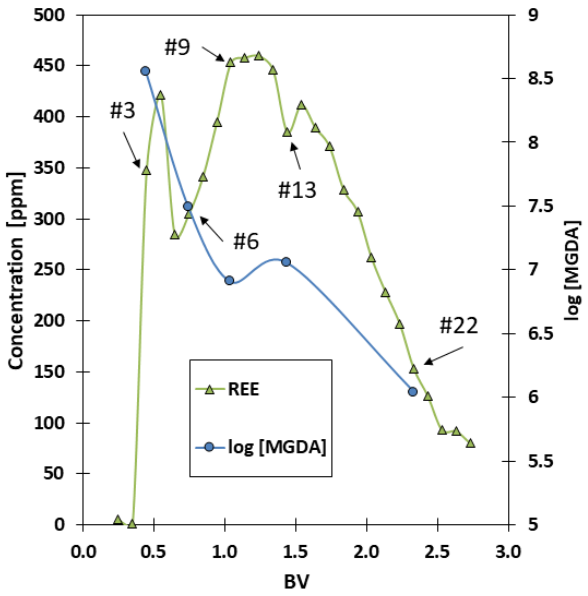

Figure 10. Chromatogram of the experiment as ∑REE with the corresponding logarithmic values of [MGDA]. (flowrate = 2.98 BV/h; feed (#2) = 0.05 BV, eluent = 50 mM HCl; T = 20 °C).

The amount of free MGDA was also measured from different experiments with different conditions. The amount of free MGDA was also measured from other experiments. The trend in all measurements complies with the findings seen in Figure 11. From those results, it can be concluded that practically all the MGDA that was observed in its free form was seen at the beginning of the chromatogram. This indicates that all the excess MGDA and MGDA–REE complexes that have not sorbed to the resin are seen as the first, narrow peak of the chromatogram. These results also indicate that the separation of REEs is based on the MGDA–REE complex; it has been shown to remain intact during the process. Almost the same amount of free MGDA was observed from a 1:4 (metal:ligand) ratio feed as from a 1:1 ratio feed. Excess MGDA is sorbed to the resin, converting the resin to the MGDA form. The REE–MGDA complex with other stoichiometry than 1:1 (M:L) cannot be excluded as an option for excess MGDA, but it is unlikely, and therefore the other M:L ratios (e.g., 1:2) were not investigated. It was seen that either the MGDA form resin or different complex structures affected the retention behavior significantly with a 1:4 (M:L) feed, as seen in Section 3.2.4.

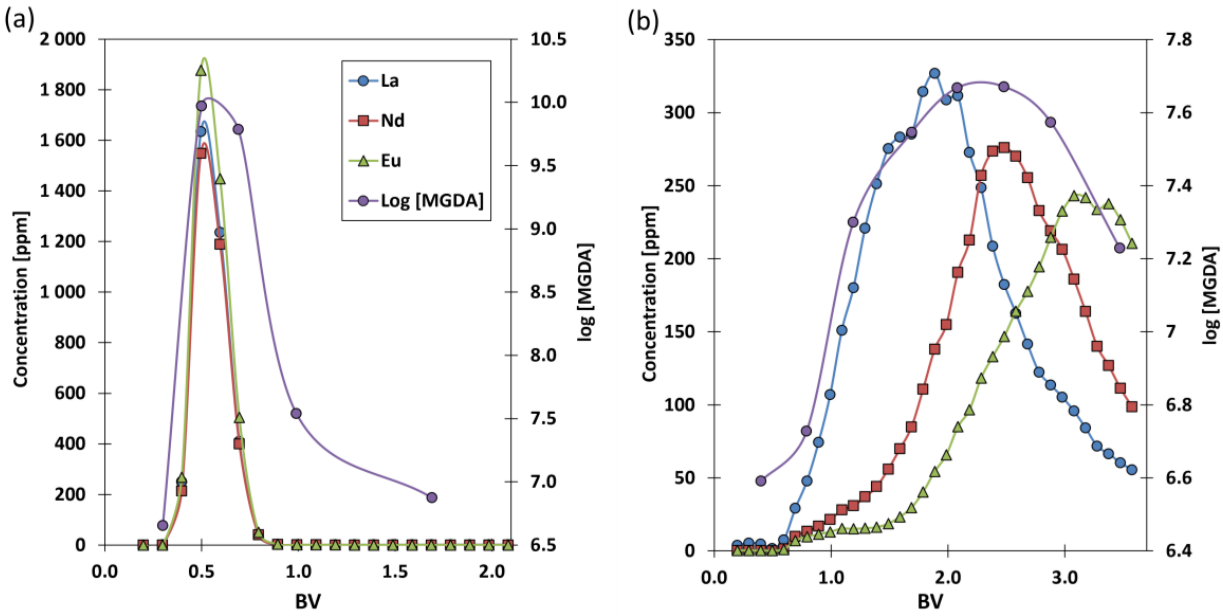

Figure 11. Chromatograms of the two-step process with separate loading and elution steps. In addition to [REE], the logarithmic [MGDA] is shown (T = 298 K ± 2 K; flowrate = 2.98 BV/h; feed (#2) = 0.1 BV; eluent = (**a**) deionized water, (**b**) 0.01 M HCl).

Adjusting the pH of the feed was not shown to affect the amount of free MGDA. The major change observed was the change in the MGDA–REE complex retention, as shown in Section 3.2.3. With elevated temperatures, the significant difference in the concentration profile of free MGDA was not seen either. Relative amounts of free MGDA experiments with temperatures of 22 °C and 50 °C are shown in Figure S4. Increasing the temperature enhances the sorption of the MGDA–REE complexes but does not affect the amount of free MGDA. Finally, the same MGDA determination was performed for a two-step process. Figure 11 shows the chromatogram for this experiment with a logarithmic presentation of free MGDA. According to previous analyses and hypotheses based on those experiments, the highest amount of MGDA was expected, as would be seen to occur in the first step of the process; this occurred as expected. For the second step, MGDA was at a similar level to the levels in the other experiments. This proposed two-step process was not practical for actual separation, but it can be used to prove the distribution of free MGDA in the system. Since the majority of free MGDA is eluted among the first peak while eluting the feed with water, it can be shown that the propagation of free MGDA is not affected by the HCl.

Although the majority of detectable free MGDA existed in a few fractions at the beginning of the chromatogram, it was also present in other samples. This small amount of MGDA after the frontal peak correlates well with the Σ[REE]. This clear connection in all the experiments can be explained by the equilibrium of the complexation reactions. For chelating reactions between strong ligands and multivalent metal cations, the equilibrium is heavily on the side of the complexes. Even though the complexation phenomenon is strong by nature, a small percentage of the metal cation and MGDA exists in the sample fractions as free species. The amount of free MGDA is presented as a logarithmic value based on relative surface areas obtained from the LC–MS analyses.

3.4. Process Performance

A total of 21 separation experiments were performed in this study with the IRA-410 resin, using different feed solutions, feed volumes, and different conditions to study the separation of REEs as MGDA complexes. This publication presents data for 10 of those experiments in the figures and discusses the results. Data from the experiments not shown does not provide any new information, which could be helpful to explain the chemistry or performance of the proposed system. From the experiments that were conducted multiple times, the reproducibility of separation can be evaluated, which is good. This data is used to analyze process performance in this section, even though the experiments were not specifically designed to optimize the process.

In ternary and multicomponent chromatographic systems, the recovery of the intermediate eluting compounds (here Nd) is always the greatest challenge. The high purity required for each metal in the corresponding product fraction leads to a trade-off between recovery yields and purities of the adjacent compounds. As observed in the chromatographic data presented above, Nd always overlaps with the adjacent La and Eu peaks. With suitable feed pH adjustments (see Section 3.2.3), the La can be separated from Nd and Eu with good purity and yield. The challenge with Eu fractions is their low concentration due to their broad elution profile. However, high purity levels can be achieved.

Figure 12 gives an example of the tradeoffs between recovery yield and product purity for each metal. The first fractionation cut, Cut_1, refers to the end of the La product fraction (its beginning is obvious and is not considered). Since no to-be-recycled or waste fractions are considered here, Cut_1 is also the beginning of the Nd product fraction. The width of the Nd fraction equals Cut_2-Cut_1, where Cut_2 is the beginning of the Eu product fraction. The end of the Eu fraction should be when it is completely eluted. With this fractionation strategy, the purity and yield of La and Eu can be presented as a single-parameter curve, whereas the data for Nd is presented as contour lines in a coordinate system spanned by the start of Nd fraction (Cut_1) and its width ($Cut_2 - Cut_1$).

Figure 12 shows that setting Cut_1 = 0.84 BV results in 81% purity and 80% yield for La. Cutting a little later (Cut_1 = 1.1 BV) increases the La yield to 89%, but the purity decreases to 70%. This is, nevertheless, a good result for a single process step in a ternary REE mixture, considering that the feed purity is approximately 33% for each metal.

The contour plots in Figure 12 show that the maximum yield and purity for Nd are not obtained with the same fractionation cut times. To obtain higher than 60% purity for Nd, Cut1 should occur between approximately 0.95 BV and 1.1 BV, and the fraction should not be wider than approximately 0.7 BV. In this range, the recovery yield is less than 50%. Decreasing the purity from 60% to 50% by collecting more Eu in the Nd fraction (Cut_1 = 0.95 BV, $Cut_2 - Cut_1$ = 1.5 BV) increases the Nd yield to 75%. This does, however, decrease the yield of Eu from 75% to 43%, while its purity increases from approximately 70% to 80%.

In many of the experiments discussed above, a large amount of non-separated REE–MGDA complexes were eluted at the void volume of the column. This "frontal peak" could be collected separately and recycled back to the feed without a loss of yield or purity. The yields and purities of all REEs could be significantly improved by using the so-called steady-state recycling chromatography [45]. In this process, low-purity fractions are collected between

the product fractions and recycled to the feed. Both recycling schemes would likely require adjustment of the pH to alkaline, thereby increasing the consumption of the acid.

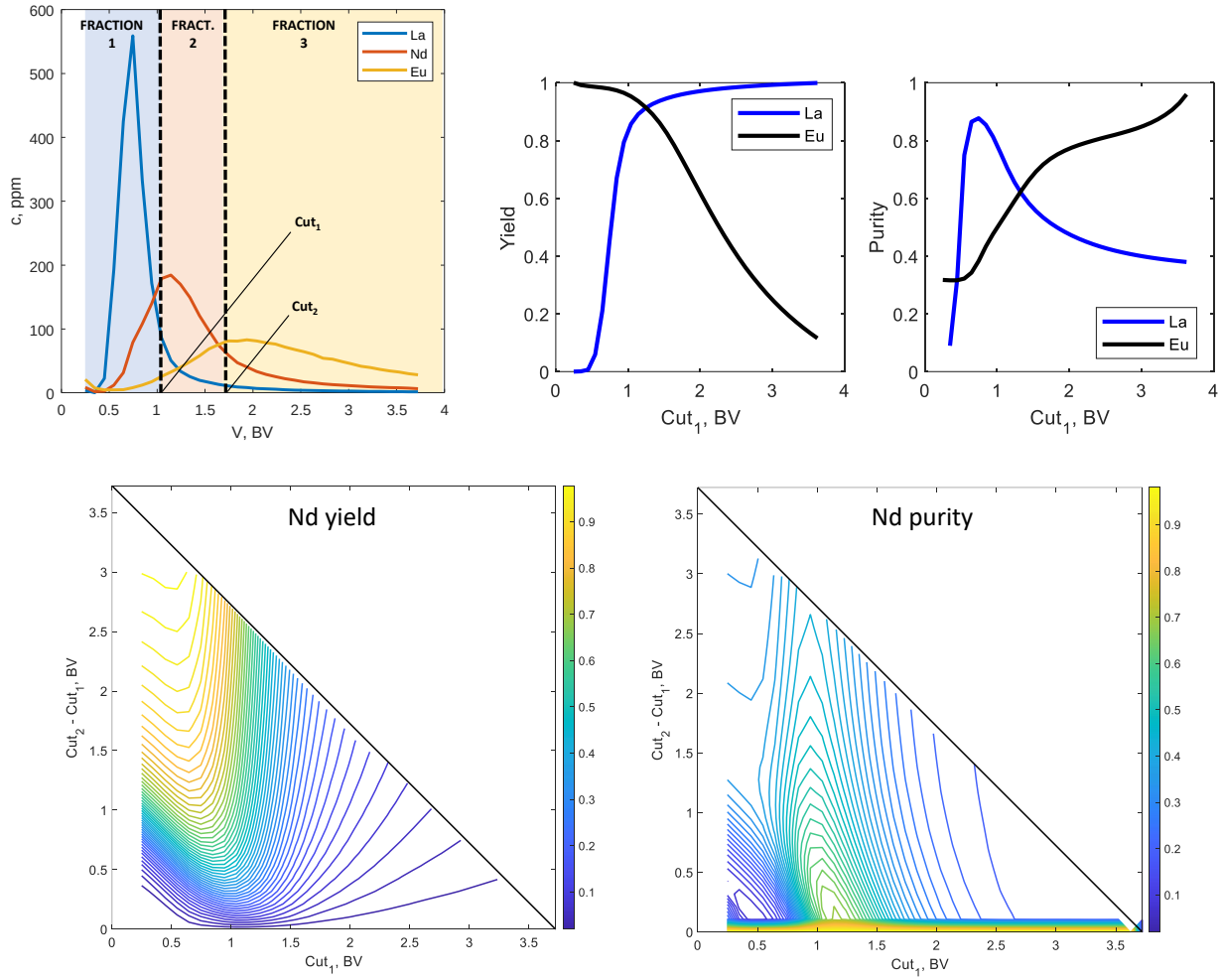

Figure 12. Effect of fractionation cut times on purity and yield of each REE (Resin = IRA-410; T = 298 ± 2 K; flowrate = 2.98 BV/h; Feed solution = #3; Feed volume = 0.025 BV; Acid concentration = 10 mM).

4. Conclusions

This study shows that MGDA–REE complexes can be chromatographically separated with SBA resin. The lower cross-linking density of the SBA resin enhances the affinity and separation; Type II dimethylethanolamine functional SBA resins perform better than Type I quaternary ammonium functional resins. Dilute strong mineral acid was shown to be a suitable eluent. HCl was chosen as the mobile phase because it does not have the unwanted interactions compared to the other alternatives (a strong interaction of HSO_4^- and SO_4^{2-} towards SBA resins and HNO_3 induces nitration of the resin matrix).

Separation of MGDA–REE complexes is based on the minor differences between the pKa values of the complexes. Since the desorption and overall separation efficiency was shown to be dependent on the pH of the system, the pH control must be precise. With 0.01 M HCl, good separation of MGDA–REE (REE = La, Nd, Eu) complexes with equivalent concentrations in the initial feed was obtained.

The purity and yield for individual REEs can be carefully controlled by choosing a proper fractionation ("cutting") scheme. The main challenge is in recovering the middle-eluting Nd in sufficient purity and yield. The following purities (P) and yields (Y) were achieved in single column separation: La, P = 81% and Y = 79%; Nd, P = 57% and Y = 65%; and Eu, P = 76% and Y = 64%.

The chemistry of the system was discussed and studied experimentally. It is concluded that the essential phenomena from a separation chemistry point of view are strong MGDA–REE complexation, protonation of MGDA (pH), and competition of chloride, dissociated free MGDA, and anionic MGDA–REE complexes for the functional groups in the resin.

Separation could be further improved by utilizing gradient elution, adding multiple consecutive stages to the system, and/or utilizing advanced process schemes such as steady-state recycling chromatography. Overall, it was demonstrated that one can modify the mobile phase composition to improve the separation significantly. This enables the use of standard commercial anion exchange resins for such a challenging separation. Ion exchange with a properly modified mobile phase could be used for separation of REEs originating from an industrial resin-in-leach process where REEs are extracted from phosphogypsum and eluted from the resin with alkaline MGDA.

Supplementary Materials: The following supporting information can be downloaded at: https://www.mdpi.com/article/10.3390/met13030600/s1, Figure S1. pH profile of the water loading step of the two-step process. The pH of pure deionized water used in loading is shown as reference. (T = 298 K ± 2 K; flowrate = 2.98 BV/h; feed (#2) = 0.1 BV; eluent = deionized water). Figure S2. Small La leakage observed in the water loading step of the two-step process. Magnification of the a) picture from Figure 11. Figure S3. Mass spectrum of the pure MGDA-Na_3 feed. (Column = Waters Acquity Premier HSS T3; injection size = 10 µL; T (column) = 303 K; mobile phase = MeOH + 0.1% FA, H_2O + 0.1% FA (60:40), flow rate = 0.2 mL/min; run time 3 + 1 min; sample = 20 µg/L MGDA (in H_2O)). Figure S4. Relative amounts of free MGDA in different fractions from experiments with temperatures of 22 °C and 50 °C.

Author Contributions: Conceptualization, S.K., S.V. and T.S.; methodology, S.V. and T.S.; formal analysis, S.K. and S.V.; investigation, S.K.; resources, S.V. and T.S.; data curation, S.K.; writing—original draft preparation, S.K.; writing—review and editing, S.V. and T.S.; visualization, S.K.; supervision, S.V. and T.S.; project administration, S.V. and T.S.; funding acquisition, S.V. and T.S. All authors have read and agreed to the published version of the manuscript.

Funding: The research was funded by the The Foundation for Research of Natural Resources in Finland, grant number 2019043. The APC was funded by LUT University.

Data Availability Statement: The data presented in this study are available within the article.

Acknowledgments: Funding from Suomen Luonnonvarain Tutkimussäätiö (The Foundation for Research of Natural Resources in Finland) is gratefully acknowledged.

Conflicts of Interest: The authors declare no conflict of interest. The funders had no role in the design of the study; in the collection, analyses, or interpretation of data; in the writing of the manuscript; or in the decision to publish the results.

References

1. Giunta, C.J.; Mainz, V.V.; Girolami, G.S. (Eds.) *50 Years of the Periodic Table Perspectives on the History of Chemistry*; Springer: Cham, Switzerland, 2021; ISBN 9783030679095.
2. Schwerdtfeger, P.; Smits, O.R.; Pyykkö, P. The Periodic Table and the Physics That Drives It. *Nat. Rev. Chem.* **2020**, *4*, 359–380. [CrossRef]
3. Yin, X.; Wang, Y.; Bai, X.; Wang, Y.; Chen, L.; Xiao, C.; Diwu, J.; Du, S.; Chai, Z.; Albrecht-Schmitt, T.E.; et al. Rare Earth Separations by Selective Borate Crystallization. *Nat. Commun.* **2017**, *8*, 14438. [CrossRef] [PubMed]
4. Reddy, B.R.; Kumar, J.R. Rare Earths Extraction, Separation, and Recovery from Phosphoric Acid Media. *Solvent Extr. Ion Exch.* **2016**, *34*, 226–240. [CrossRef]
5. Campbell, D.S. Chromatographic Lanthanide Separations Using a High-Pressure Ion Exchange Method. *Ind. Eng. Chem. Process Des. Dev.* **1970**, *9*, 89–94. [CrossRef]
6. Dybczyński, R.S.; Pyszynska, M.; Kulisa, K.; Bojanowska-Czajka, A. Selective Separation of Yttrium from Rare Earth Elements by Ion Interaction Chromatography. Analytical and Larger Scale Applications. *Sep. Sci. Technol.* **2020**, *55*, 1364–1379. [CrossRef]
7. Chi, R.; Xu, Z. Solution Chemistry Approach to the Study of Rare Earth Element Precipitation by Oxalic Acid. *Metall. Mater. Trans. B* **1999**, *30*, 189–195. [CrossRef]
8. Han, K.N. Characteristics of Precipitation of Rare Earth Elements with Various Precipitants. *Minerals* **2020**, *10*, 178. [CrossRef]
9. Xie, F.; Zhang, T.A.; Dreisinger, D.; Doyle, F. A Critical Review on Solvent Extraction of Rare Earths from Aqueous Solutions. *Miner. Eng.* **2014**, *56*, 10–28. [CrossRef]

10. Kuchi, R.; Kim, D. Rare Earth-Based Magnetic Materials: Progresses in the Fabrication Technologies and Magnetic Properties. In *Rare-Earth Metal Recovery for Green Technologies*; Springer: Cham, Switzerland, 2020; ISBN 9783030381059.
11. Kuang, S.T.; Liao, W.P. Progress in the Extraction and Separation of Rare Earths and Related Metals with Novel Extractants: A Review. *Sci. China Technol. Sci.* **2018**, *61*, 1319–1328. [CrossRef]
12. Sun, X.; Waters, K.E. Development of Industrial Extractants into Functional Ionic Liquids for Environmentally Friendly Rare Earth Separation. *ACS Sustain. Chem. Eng.* **2014**, *2*, 1910–1917. [CrossRef]
13. Ashour, R.M.; Samouhos, M.; Polido Legaria, E.; Svärd, M.; Högblom, J.; Forsberg, K.; Palmlöf, M.; Kessler, V.G.; Seisenbaeva, G.A.; Rasmuson, Å.C. DTPA-Functionalized Silica Nano- and Microparticles for Adsorption and Chromatographic Separation of Rare Earth Elements. *ACS Sustain. Chem. Eng.* **2018**, *6*, 6889–6900. [CrossRef]
14. Dong, Z.; Mattocks, J.A.; Deblonde, G.J.P.; Hu, D.; Jiao, Y.; Cotruvo, J.A.; Park, D.M. Bridging Hydrometallurgy and Biochemistry: A Protein-Based Process for Recovery and Separation of Rare Earth Elements. *ACS Cent. Sci.* **2021**, *7*, 1798–1808. [CrossRef]
15. Arrigo, L.M.; Jiang, J.; Finch, Z.S.; Bowen, J.M.; Beck, C.L.; Friese, J.I.; Greenwood, L.R.; Seiner, B.N. Development of a Separation Method for Rare Earth Elements Using LN Resin. *J. Radioanal. Nucl. Chem.* **2021**, *327*, 457–463. [CrossRef]
16. Wang, Y.; Gong, A.; Qiu, L.; Zhang, W.; Traore, M.; Bai, Y.; Liu, Y.; Gao, G.; Zhao, W.; Qin, W.; et al. Preparation of Pyrrolidinyl Diglycolamide Bonded Silica Particles and Its Rare Earth Separation Properties. *J. Chromatogr. A* **2022**, *1681*, 463396. [CrossRef]
17. Settle, F.A. Analytical Chemistry and the Manhattan Project. *Anal. Chem.* **2002**, *74*, 36A–43A. [CrossRef]
18. Johnson, W.C.; Quill, L.L.; Daniels, F. Rare Earths Separation Developed on Manhattan Project. *Chem. Eng. News* **1947**, *25*, 2494. [CrossRef]
19. Ramzan, M.; Kifle, D.; Wibetoe, G. Comparative Study of Stationary Phases Impregnated with Acidic Organo-phosphorus Extractants for HPLC Separation of Rare Earth Elements. *Sep. Sci. Technol.* **2016**, *51*, 494–501. [CrossRef]
20. Traore, M.; Gong, A.; Wang, Y.; Qiu, L.; Bai, Y.; Zhao, W.; Liu, Y.; Chen, Y.; Liu, Y.; Wu, H.; et al. Research Progress of Rare Earth Separation Methods and Technologies. *J. Rare Earths* **2022**, *41*, 182–189. [CrossRef]
21. Dembowski, M.; Rowley, J.E.; Boland, K.; Droessler, J.; Hathcoat, D.A.; Marchi, A.; Goff, G.S.; May, I. Rare Earth Element Separations by High-Speed Counter-Current Chromatography. *J. Chromatogr. A* **2022**, *1682*, 463528. [CrossRef]
22. Spedding, F.H.; Powell, J.E.; Wheelwright, E.J. The Separation of Adjacent Rare Earths with Ethylenediamine-Tetraacetic Acid by Elution from an Ion-Exchange Resin. *J. Am. Chem. Soc.* **1954**, *72*, 612–613. [CrossRef]
23. Ling, L.; Wang, N.H.L. Ligand-Assisted Elution Chromatography for Separation of Lanthanides. *J. Chromatogr. A* **2015**, *1389*, 28–38. [CrossRef] [PubMed]
24. Chen, B.; He, M.; Zhang, H.; Jiang, Z.; Hu, B. Chromatographic Techniques for Rare Earth Elements Analysis. *Phys. Sci. Rev.* **2019**, *2*, 20160057. [CrossRef]
25. Li, J.; Gong, A.; Qiu, L.; Zhang, W.; Shi, G.; Li, X.; Li, J.; Gao, G.; Bai, Y. Selective Extraction and Column Separation for 16 Kinds of Rare Earth Element Ions by Using *N*,*N*-Dioctyl Diglycolacid Grafted Silica Gel Particles as the Stationary Phase. *J. Chromatogr. A* **2020**, *1627*, 461393. [CrossRef] [PubMed]
26. Fernández, R.G.; Alonso, J.I.G. Separation of Rare Earth Elements by Anion-Exchange Chromatography Using Ethylenediaminetetraacetic Acid as Mobile Phase. *J. Chromatogr. A* **2008**, *1180*, 59–65. [CrossRef] [PubMed]
27. Kharitonov, O.V.; Firsova, L.A.; Kostikova, G.V.; Zhilov, V.I. Separation of TPE and REE by Displacement Chelating Chromatography in the Presence of Iron, Chromium and Aluminum Impurities. *Radiochemistry* **2022**, *64*, 618–624. [CrossRef]
28. Opare, E.O.; Struhs, E.; Mirkouei, A. A Comparative State-of-Technology Review and Future Directions for Rare Earth Element Separation. *Renew. Sustain. Energy Rev.* **2021**, *143*, 110917. [CrossRef]
29. Sungur, Ş.K.; Akseli, A. Separation and Determination of Rare Earth Elements by Dowex 2-X8 Resin Using Sodium Trimetaphosphate as Elution Agent. *J. Chromatogr. A* **2000**, *874*, 311–317. [CrossRef]
30. Knutson, H.K.; Max-Hansen, M.; Jönsson, C.; Borg, N.; Nilsson, B. Experimental Productivity Rate Optimization of Rare Earth Element Separation through Preparative Solid Phase Extraction Chromatography. *J. Chromatogr. A* **2014**, *1348*, 47–51. [CrossRef]
31. Dybczyński, R.S.; Kulisa, K. Separation of Rare Earth Elements (REE) by Ion Interaction Chromatography (IIC) Using Diglycolic Acid (ODA) as a Complexing Agent. *Chromatographia* **2021**, *84*, 473–482. [CrossRef]
32. Kurkinen, S.; Virolainen, S.; Sainio, T. Recovery of Rare Earth Elements from Phosphogypsum Waste in Res-in-in-Leach Process by Eluting with Biodegradable Complexing Agents. *Hydrometallurgy* **2021**, *201*, 105569. [CrossRef]
33. Migdisov, A.A.; Williams-Jones, A.E. A Spectrophotometric Study of Neodymium(III) Complexation in Chloride Solutions. *Geochim. Cosmochim. Acta* **2002**, *66*, 4311–4323. [CrossRef]
34. DuPont Ion Exchange Resins Selectivity. Available online: https://www.dupont.com/content/dam/dupont/amer/us/en/water-solutions/public/documents/en/IER-Selectivity-TechFact-45-D01458-en.pdf (accessed on 1 July 2022).
35. Nouryon MGDA Technical Brochure Dissolvine®M-40 Dissolvine®M-S. Available online: https://www.nouryon.com/globalassets/inriver/resources/brochure-home-care-dissolvine-m40-ms-global-en.pdf (accessed on 1 July 2022).
36. Wódkiewicz, L.; Dybczynski, R. Effect of Resin Cross-Linking on the Anion-Exchange Separation of Rare Earth Complexes with DCTA. *J. Chromatogr.* **1972**, *68*, 131–141. [CrossRef]
37. Hubicka, H.; Drobek, D. Separation of Y(III) Complexes from Dy(III), Ho(III) and Er(III) Complexes with Iminodiacetic Acid on the Anion-Exchangers Type 1 and Type 2. *Hydrometallurgy* **1999**, *53*, 89–100. [CrossRef]
38. Dron, J.; Dodi, A. Thermodynamic Modeling of Cl^-, NO_3^- and SO_4^{2-} Removal by an Anion Exchange Resin and Comparison with Dubinin-Astakhov Isotherms. *Langmuir* **2011**, *27*, 2625–2633. [CrossRef]

39. Jachuła, J.; Kołodyńska, D.; Hubicki, Z. Sorption of Cd(II), Co(II), and Zn(II) Complexes with MGDA on Anion Exchange Resins: A Study of the Influence of Various Parameters. *Sep. Sci. Technol.* **2013**, *48*, 1801–1809. [CrossRef]
40. Kołodyńska, D.; Hubicka, H.; Hubicki, Z. Studies of Application of Monodisperse Anion Exchangers in Sorption of Heavy Metal Complexes with IDS. *Desalination* **2009**, *239*, 216–228. [CrossRef]
41. Salvatella, L. The Alkyl Group Is a −I + R Substituent. *Educ. Quim.* **2017**, *28*, 232–237. [CrossRef]
42. Solov'ev, V.; Varnek, A. Thermodynamic Radii of Lanthanide Ions Derived from Metal–Ligand Complexes Stability Constants. *J. Incl. Phenom. Macrocycl. Chem.* **2020**, *98*, 69–78. [CrossRef]
43. Fritz, J.S. Factors Affecting Selectivity in Ion Chromatography. *J. Chromatogr. A* **2005**, *1085*, 8–17. [CrossRef]
44. Hyvönen, H. *Studies on Metal Complex Formation of Environmentally Friendly Aminopolycarboxylate Chelating Agents*; Helsingin Yliopisto: Helsinki, Finland, 2008; ISBN 9789529240050.
45. Kaspereit, M.; Sainio, T. Simplified Design of Steady-State Recycling Chromatography under Ideal and Nonideal Conditions. *Chem. Eng. Sci.* **2011**, *66*, 5428–5438. [CrossRef]